Inorg. Chem. **2002**, *41*, 2633–2641

Cyclometalated Products of $[(COE)_2RhCl]_2$ and 1,3-$(RSCH_2)_2C_6H_4$ (R = ^{t}Bu, ^{i}Pr) Are Dimeric. Synthesis, Molecular Structures, and Solution Dynamics of $[\mu$-ClRh(H)$(RSCH_2)_2C_6H_3$-2,6$]_2$

Daniel R. Evans,*,† Mingsheng Huang,† W. Michael Seganish,† Esther W. Chege,† Yiu-Fai Lam,† James C. Fettinger,† and Tracie L. Williams‡

Department of Chemistry and Biochemistry, University of Maryland, College Park, Maryland 20742, and Center for Food Safety and Nutrition, 5100 Paint Branch Parkway, College Park, Maryland 20740

Received November 21, 2001

Two tridentate thioether pincer ligands, 1,3-$(RSCH_2)_2C_6H_4$ (R = ^{t}Bu, **1a**; R = ^{i}Pr, **1b**) underwent cyclometalation using $[(COE)_2RhCl]_2$ in air/moisture-free benzene at room temperature. The resultant complexes, $[\mu$-ClRh(H)-$(RSCH_2)_2C_6H_3$-2,6$]_2$ (R = ^{t}Bu, **2a**; R = ^{i}Pr, **2b**) are dimeric both in the solid state and in solution. A battery of variable-temperature one- and two-dimensional ^{1}H NMR experiments showed conclusively that both complexes undergo dynamic exchange in solution. Exchange between two dimeric diastereomers of **2a** in solution occurred via rotation about the Rh–C_{ipso} bond. The dynamic exchange of **2b** was significantly more complex as an additional exchange mechanism, sulfur inversion, occurred, which resulted in the exchange between several diastereomers in solution.

Introduction

Initial reports that utilized the anionic tridentate "pincer" ligand (LCL^-) appeared some time ago.[1] This ligand framework received further attention due to its ability to chelate a wide array of transition metals. Unlike other spectator ligands commonly encountered in organometallic chemistry (Cp^-, Tp^-, TACN, etc.) that coordinate metals facially, the pincer ligands coordinate metals meridonally in which the two pendant ligands are situated trans to each other.

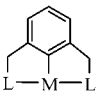

2,6-$(LCH_2)_2C_6H_3M$
L = NR_2, PR_2, SR, NR_1R_2, $P(O)R_2$, S(O)R

This bonding arrangement is ideal in many respects as it provides stable chelates and exploits the strong trans effect of C_{ipso} to provide very active homogeneous catalysts. Another attractive feature of these systems is that a wide array of chelating auxiliaries is possible with a multitude of properties. For example, amino- and phosphino-containing pincer ligands (L = NR_2, PR_2) chelate metals spanning the entire periodic table.[2] Examination of pincer complexes (L = NR_2 (M = Pt), PR_2 (M = Rh)) provided important clues as to the nature of cyclometalation.[3] A pincer ligand (L = NR_2) presented an opportunity to study the elusive silyl cation,[4] while another system (L = $P(O)R_2$) afforded a glimpse into the reactivity of penta- and hexacoordinate Sn(IV) adducts.[5] Other pincer−metal complexes exhibit extraordinary thermal stability and catalyze alkane dehydrogenation,[6a,b] Kharasch,[6c] and Suzuki reactions,[2k] while palladium−pincers,[6d−h] (L = PR_2, SR) are extremely active Heck catalysts. Several examples exist in which the introduction of chiral elements provided pincer−metal complexes capable of enantioselective catalysis.[7] Finally, thioether-based pincer complexes, when ligated with Pd(II), either function as unique small molecule receptors[8] or serve as templates for supramolecular assemblies.[9] Our own contribution showed that incorporation of the rarely studied sulfoxide within this framework provided stable chelates of Pd(II).[10]

* Corresponding author. Telephone: (301) 405-8436. Fax: (301) 314-9121. E-mail: de44@umail.umd.edu.
† University of Maryland.
‡ CFSAN/FDA.

(1) (a) Moulton, C. J.; Shaw, B. L. *J. Chem. Soc., Dalton Trans.* **1976**, 1020−1024. (b) Van Koten, G.; Timmer, K.; Noltes, J. G.; Spek, A. L. *J. Chem. Soc., Chem. Commun.* **1978**, 250−252. (c) Nemeh, S.; Jensen, C.; Binamira-Soriaga, E.; Kaska, W. C. *Organometallics* **1983**, *2*, 1442−1447. (d) Rimml, H.; Venanzi, L. M. *J. Organomet. Chem.* **1983**, *259*, C6−C7. (e) Grove, D. M.; van Koten, G.; Ubbels, H. J. C.; Zoet, R.; Spek, A. L. *Organometallics* **1984**, *3*, 1003−1009.

10.1021/ic011189y CCC: $22.00
Published on Web 04/19/2002

To date, the only known examples of thioether-based pincer ligand complexes involve chelation to the heavier metals of group 10.[8,9,11] Our research program comprises the examination of new ligand systems as applied to homogeneous catalysis.[10] Considering the utility of R(LCL)M systems examined thus far, and the importance of group 9 metals as catalytically active metals, our desire is to explore the chemistry of R(SCHS) in conjunction with Rh and Ir. Herein, we wish to report the first example of R(SCS) ligation to Rh(III).

Scheme 1

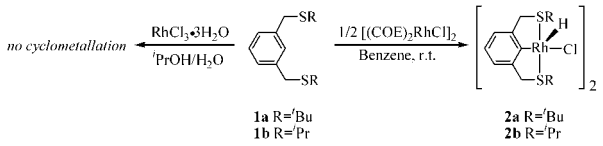

Results and Discussion

Synthesis of Ligands and Complexes. Several reports adequately describe the synthesis of the requisite starting material, 1,3-$(RSCH_2)_2C_6H_4$, R(SCHS) (**1a**, R = ^{t}Bu; **1b**, R = ^{i}Pr);[8,9,11] however, the availability of reagents prompted an alternative formulation. Preparation of **1** proceeded in one step upon reaction of a stoichiometric amount of RSNa with 1,3-$(ClCH_2)_2C_6H_4$ in DMF at 100 °C (eq 1). The procedure

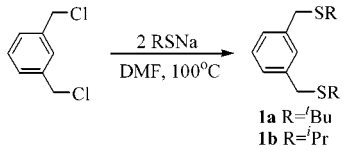

(1)

resulted in the isolation of **1a** as fine off-white needles and **1b** as a colorless liquid in isolated yields of 82% and 87%, respectively. ^{1}H NMR and HR-FAB-MS yielded data that were consistent with the formulated species.

Two general procedures exist for the preparation of Rh−pincer complexes; both depend on the presence of Rh(I), Scheme 1. The first method generates Rh(I) in situ in refluxing isopropyl alcohol/water solution starting with $RhCl_3 \cdot 3H_2O$ with subsequent addition of an excess of R(LCHL).[1a] All attempts to utilize this method for the metalation of **1** repeatedly failed. Indeed, addition of ligand to the reaction solution always resulted in the formation of an orange-yellow solid that was insoluble in most organic solvents. The solid dissolved upon heating in d_6-DMSO, but inspection of the ^{1}H NMR spectrum revealed **1** as the only species in solution. Previous work noted that oligomeric adducts, or "large ring systems", of arene-free pincer ligands form under these conditions rather than the desired cyclometalated species.[12] Therefore, under these reaction conditions, the process of oligomerization is apparently favored rather than cyclometalation.

(2) (a) Dekoster, A.; Kanters, J. A.; Spek, A. L.; Vanderzeijden, A. A. H.; Van Koten, G.; Vrieze, K. *Acta Crystallogr., Sect. C: Cryst. Struct. Commun.* **1985**, *41*, 893−895. (b) Abbenhuis, H. C. L.; Feiken, N.; Grove, D. M.; Jastrzebski, J.; Kooijman, H.; Vandersluis, P.; Smeets, W. J. J.; Spek, A. L.; Van Koten, G. *J. Am. Chem. Soc.* **1992**, *114*, 9773−9781. (c) Bennett, M. A.; Jin, H.; Willis, A. C. *J. Organomet. Chem.* **1993**, *451*, 249−256. (d) Olazabal, C. A.; Gabbai, F. P.; Cowley, A. H.; Carrano, C. J.; Mokry, L. M.; Bond, M. R. *Organometallics* **1994**, *13*, 421−423. (e) Cross, R. J.; Kennedy, A. R.; Manojlovicmuir, L.; Muir, K. W. *J. Organomet. Chem.* **1995**, *493*, 243−249. (f) Sutter, J. P.; James, S. L.; Steenwinkel, P.; Karlen, T.; Grove, D. M.; Veldman, N.; Smeets, W. J. J.; Spek, A. L.; van Koten, G. *Organometallics* **1996**, *15*, 941−948. (g) Hogerheide, M. P.; Boersma, J.; Spek, A. L.; van Koten, G. *Organometallics* **1996**, *15*, 1505−1507. (h) Bonnardel, P. A.; Parish, R. V.; Pritchard, R. G. *J. Chem. Soc., Dalton Trans.* **1996**, 3185−3193. (i) van der Boom, M. E.; Kraatz, H.-B.; Hassner, L.; Ben-David, Y.; Milstein, D. *Organometallics* **1999**, *18*, 3873−3884. (j) Brandts, J. A. M.; Kruiswijk, E.; Boersma, J.; Spek, A. L.; van Koten, G. *J. Organomet. Chem.* **1999**, *585*, 93−99. (k) Weissman, H.; Milstein, D. *Chem. Commun.* **1999**, 1901−1902. (l) Gauvin, R. M.; Rozenberg, H.; Shimon, L. J. W.; Milstein, D. *Organometallics* **2001**, *20*, 1719−1724. (m) Hughes, R. P.; Williamson, A.; Incarvito, C. D.; Rheingold, A. L. *Organometallics* **2001**, *20*, 4741−4744.

(3) (a) Terheijden, J.; Van Koten, G.; Vinke, I. C.; Spek, A. L. *J. Am. Chem. Soc.* **1985**, *107*, 2891−2898. (b) Canty, A. J.; Van Koten, G. *Acc. Chem. Res.* **1995**, *28*, 406−413. (c) Vigalok, A.; Uzan, O.; Shimon, L. J. W.; Ben-David, Y.; Martin, J. M. L.; Milstein, D. *J. Am. Chem. Soc.* **1998**, *120*, 12539−12544. (d) Gossage, R. A.; Ryabov, A. D.; Spek, A. L.; Stufkens, D. J.; van Beek, J. A. M.; van Eldik, R.; van Koten, G. *J. Am. Chem. Soc.* **1999**, *121*, 2488−2497. (e) Gandelman, M.; Vigalok, A.; Konstantinovski, L.; Milstein, D. *J. Am. Chem. Soc.* **2000**, *122*, 9848−9849. (f) Albrecht, M.; Spek, A. L.; van Koten, G. *J. Am. Chem. Soc.* **2001**, *123*, 7233−7246. (g) Albrecht, M.; Spek, A. L.; van Koten, G. *J. Am. Chem. Soc.* **2001**, *123*, 7233−7246.

(4) Chauhan, M.; Chuit, C.; Corriu, R. J. P.; Mehdi, A.; Reye, C. *Organometallics* **1996**, *15*, 4326−4333.

(5) Mehring, M.; Schurmann, M.; Jurkschat, K. *Organometallics* **1998**, *17*, 1227−1236.

(6) (a) Liu, F.; Pak, E. B.; Singh, B.; Jensen, C. M.; Goldman, A. S. *J. Am. Chem. Soc.* **1999**, *121*, 4086−4087. (b) Jensen, C. M. *Chem. Commun.* **1999**, 2443−2449, and references therein. (c) Gossage, R. A.; Van De Kuil, L. A.; Van Koten, G. *Acc. Chem. Res.* **1998**, *31*, 423−431. (d) Ohff, M.; Ohff, A.; van der Boom, M. E.; Milstein, D. *J. Am. Chem. Soc.* **1997**, *119*, 11687−11688. (e) Morales-Morales, D.; Redon, R.; Yung, C.; Jensen, C. M. *Chem. Commun.* **2000**, 1619−1620. (f) Morales-Morales, D.; Grause, C.; Kasaoka, K.; Redon, R.; Cramer, R. E.; Jensen, C. M. *Inorg. Chim. Acta* **2000**, *300*−*302*, 958−963. (g) Bergbreiter, D. E.; Osburn, P. L.; Liu, Y.-S. *J. Am. Chem. Soc.* **1999**, *121*, 9531−9538. (h) Gruber, A. S.; Zim, D.; Ebeling, G.; Monteiro, A. L.; Dupont, J. *Org. Lett.* **2000**, *2*, 1287−1290.

(7) (a) Gorla, F.; Venanzi, L. M.; Albinati, A. *Organometallics* **1994**, *13*, 43−54. (b) Stark, M. A.; Richards, C. J. *Tetrahedron Lett.* **1997**, *38*, 5881−5884. (c) Longmire, J. M.; Zhang, X. M.; Shang, M. Y. *Organometallics* **1998**, *17*, 7, 4374−4379. (d) Stark, M. A.; Jones, G.; Richards, C. J. *Organometallics* **2000**, *19*, 1282−1291. (e) Albrecht, M.; Kocks, B. M.; Spek, A. L.; van Koten, G. *J. Organomet. Chem.* **2001**, *624*, 271−286.

(8) (a) Kickham, J. E.; Loeb, S. J. *Inorg. Chem.* **1994**, *33*, 4351−4359. (b) Kickham, J. E.; Loeb, S. J. *Inorg. Chem.* **1995**, *34*, 5656−5665. (c) Cameron, B. R.; Loeb, S. J.; Yap, G. P. A. *Inorg. Chem.* **1997**, *36*, 5498−5504. (d) Kickham, J. E.; Loeb, S. J.; Murphy, S. L. *Chem. Eur. J.* **1997**, *3*, 1203−1213.

(9) (a) Loeb, S. J.; Shimizu, G. K. H. *Chem. Commun.* **1993**, 1395−1397. (b) Huck, W. T. S.; van Veggel, F. C. J. M.; Kropman, B. L.; Blank, D. H. A.; Keim, E. G.; Smithers, M. M. A.; Reinhoudt, D. N. *J. Am. Chem. Soc.* **1995**, *117*, 8293−8294. (c) Huck, W. T. S.; Snellink-Ruel, B.; van Veggel, F.; Reinhoudt, D. N. *Organometallics* **1997**, *16*, 4287−4291. (d) Huck, W. T. S.; Prins, L. J.; Fokkens, R. H.; Nibbering, N. M. M.; van Veggel, F.; Reinhoudt, D. N. *J. Am. Chem. Soc.* **1998**, *120*, 6240−6246.

(10) Evans, D. R.; Huang, M.; Seganish, W. M.; Fettinger, J. C.; Williams, T. L. *Organometallics*, **2002**, *21*, 893−900.

(11) (a) Errington, J.; McDonald, W. S.; Shaw, B. L. *J. Chem. Soc., Dalton Trans.* **1980**, 2312−2314. (b) Dupont, J.; Beydoun, N.; Pfeffer, M. *J. Chem. Soc., Dalton Trans.* **1989**, 1715−1720. (c) Lucena, N.; Casabo, J.; Escriche, L.; Sanchez-Castello, G.; Teixidor, F.; Kivekas, R.; Sillanpaa, R. *Polyhedron* **1996**, *15*, 3009−3018. (d) Loeb, S. J.; Shimizu, G. K. H.; Wisner, J. A. *Organometallics* **1998**, *17*, 2324−2327. (e) van Manen, H. J.; Nakashima, K.; Shinkai, S.; Kooijman, H.; Spek, A. L.; van Veggel, F.; Reinhoudt, D. N. *Eur. J. Inorg. Chem.* **2000**, 2533−2540.

(12) (a) Crocker, C.; Empsall, H. D.; Errington, R. J.; Hyde, E. M.; McDonald, W. S.; Markham, R.; Norton, M. C.; Shaw, B. L.; Weeks, B. *J. Chem. Soc., Dalton Trans.* **1982**, 1217−1224. (b) Briggs, J. R.; Constable, A. G.; McDonald, W. S.; Shaw, B. L. *J. Chem. Soc., Dalton Trans.* **1982**, 1225−1230.

A recently developed method for the metalation of R(PCHP) using [(L)$_2$RhCl]$_2$ (L = COE, ethylene) seemed like an attractive alternative as it occurs under much milder conditions.[13] The reaction of **1** with [(COE)$_2$RhCl]$_2$ in benzene at room temperature for a period of 18 h, Scheme 1, provided the desired cyclometalation products, which resulted in isolated yields of 95% and 83% for **2a** and **2b**, respectively. Infrared analysis of both complexes confirmed the presence of the hydride ligand, as strong Rh−H stretches were present at 2108 (**2a**) and 2120 cm^{-1} (**2b**). ^{1}H NMR analysis of **2a** in C_6D_6 solution showed two hydride resonances, approximately 20 ppm upfield of TMS (average $^1J_{RhH}$ = 24 Hz) in a ratio of 2.2 to 1. The hydride region of **2b** was significantly more complex as at least 11 resonances appeared in the −19 to −22 ppm region. Two resonances observed at −19.93 ($^1J_{RhH}$ = 25.6 Hz) and −20.16 ($^1J_{RhH}$ = 27.6 Hz) corresponded to 23% and 45% of the total integrated intensity of the hydride region. ^{1}H NMR spectra recorded at 88 °C showed a broad coalesced hydride resonance, and suggested that the multiple resonances observed at room temperature exchanged at a rate that was slow relative to the NMR time scale of 400.132 MHz.

Crystals suitable for X-ray diffraction showed that **2** was dimeric in the solid state; see below. The immediate question to answer was whether **2** was dimeric in solution. This is important as the dynamic exchange observed by ^{1}H NMR could be a result of a monomer−dimer equilibrium. Evidence to support the formulation of **2** as a dimer in solution came from electrospray mass spectroscopy, ESI-MS. Experiments performed under a variety of conditions failed to reveal the presence of any monomer in solution. Indeed, the predominant ion present in CH_2Cl_2 solution for **2** was [**2**-Cl]$^+$. *Exclusive observation of the dimeric species provides unambiguous evidence that these complexes are dimeric in solution.*

This is an extraordinary outcome, as previous reports that used phosphine-based pincer ligands, 1,3-(R$_2$PCH$_2$)-2-R′-C$_6$H$_3$ (R = ^{t}Bu, R′ = H, Me),[1c,13] showed conclusively that the metalated adducts (R(PCP)Rh(R′)Cl) were monomeric. In these examples, the rhodium resides within a square pyramidal coordination environment in which C_{ipso} is trans to Cl, and R′ occupies the apical site. In the case where R′ = H, $^1J_{RhH}$ was a diagnostic reporter of the coordination geometry as large coupling to rhodium was observed (ca. 50 Hz).[1a,c] Further evidence to demonstrate that **2** is dimeric in solution occurred upon inspection of the observed Rh−H coupling constants. Indeed, the coupling observed in these two complexes (**2a** and **2b**) was reduced by a factor of 2, when compared to R(PCP)Rh(H)Cl, and is similar to that observed for H$_2$RhL$_2$(μ-Cl)$_2$RhL$_2$ (L = PPh$_3$).[14] Thus, unlike the related chemistry with PCP ligands, the SCS ligands result in dimeric complexes. Further corroboration of this fundamental difference resulted upon the determination of the dimeric molecular structures of both **2a** and **2b**.

Molecular Structures. ORTEP representations (50% probability) of **2a** and **2b** appear in Figures 1 and 2,

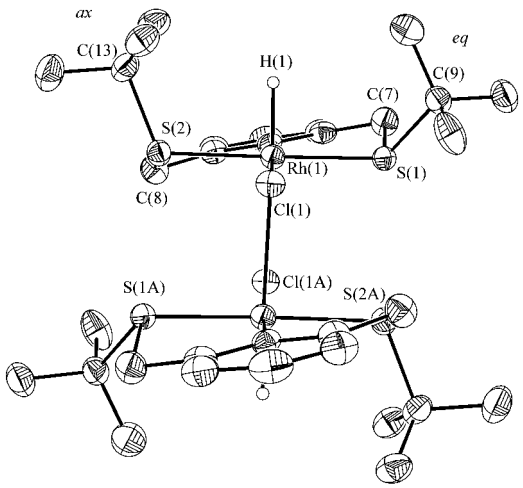

Figure 1. ORTEP representation of **2a**. Thermal ellipsoids are drawn at the 50% probability level. Benzene solvate and C−H hydrogens have been omitted for clarity. Selected bond lengths (Å) and angles (deg): Rh(1)−C(1), 1.992(3), Rh(1)−S(1), 2.2981(8); Rh(1)−S(2), 2.3087(8); Rh(1)−Cl(1), 2.5045(8); Rh(1)−Cl(1A), 2.5821(8); Rh(1)−H(1), 1.50(3); C(1)−Rh(1)−S(1), 84.42(9); C(1)−Rh(1)−S(2), 86.00(9); C(1)−Rh(1)−H(1), 87.1(12).

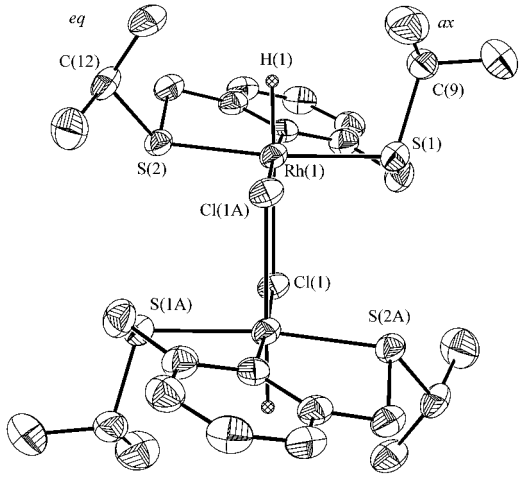

Figure 2. ORTEP representation of **2b**. Thermal ellipsoids are drawn at the 50% probability level. Benzene solvate and C−H hydrogens have been omitted for clarity. Selected bond lengths (Å) and angles (deg): Rh(1)−C(1), 1.979(3); Rh(1)−S(1), 2.3286(8); Rh(1)−S(2), 2.2975(7); Rh(1)−Cl(1), 2.5838(7); Rh(1)−Cl(1A), 2.5089(7); Rh(1)−H(1), 1.44(4); C(1)−Rh(1)−S(1), 84.58(8); C(1)−Rh(1)−S(2), 83.54(8); C(1)−Rh(1)−H(1), 85.4(14).

respectively, while Tables 1 and 2 provide selected metrical parameters and crystallographic data for both complexes. (During the course of manuscript revision, an additional structure of **2a** was determined (see Supporting Information).) The average bond distances reported herein reflect the averages of the values listed in Tables 1 and S8). The centrosymmetric dimers crystallized in either the triclinic (**2a**) or monoclinic (**2b**) crystal systems with the monomeric species being crystallographically unique. The center of symmetry for both molecules lies at the centroid of the Rh(1)−Cl(1)−Rh(1A)−Cl(1A) four-membered ring. Either benzene or methylene chloride solvates exist in both structures, depending on the solvent of crystallization.

(13) Rybtchinski, B.; Vigalok, A.; Ben-David, Y.; Milstein, D. *J. Am. Chem. Soc.* **1996**, *118*, 12406−12415.

(14) Duckett, S. B.; Newell, C. L.; Eisenberg, R. *J. Am. Chem. Soc.* **1994**, *116*, 10548−10556.

Table 1. Selected Bond Distances and Bond, Torsional (ω), and Interplanar (Ω) Angles for **2a** and **2b**

	2a	**2b**
Bond Distances, Å		
Rh(1)−C(1)	1.992(3)	1.979(3)
Rh(1)−S(1)	2.2981(8)	2.3286(8)
Rh(1)−S(2)	2.3087(8)	2.2975(7)
Rh(1)−Cl(1)	2.5045(8)	2.5838(7)
Rh(1)−Cl(1A)	2.5821(8)	2.5089(7)
Rh(1)−H(1)	1.50(3)	1.44(4)
Bond Angles, deg		
C(1)−Rh(1)−S(1)	84.42(9)	84.58(8)
C(1)−Rh(1)−S(2)	86.00(9)	83.54(8)
S(1)−Rh(1)−S(2)	170.41(3)	167.74(3)
C(1)−Rh(1)−H(1)	87.1(12)	85.4(14)
S(1)−Rh(1)−H(1)	91.2(12)	91.4(14)
S(2)−Rh(1)−H(1)	88.7(12)	84.6(14)
Cl(1)−Rh(1)−H(1)	96.7(12)	178.6(14)
Cl(1A)−Rh(1)−H(1)	176.6(12)	95.0(14)
Rh(1)−Cl(1)−Rh(1A)	94.73(3)	94.32(2)
Torsional Angles, ω,[a] deg		
H(1)−Rh−S−C_{eq}[b]	39.7	−42.0
H(1)−Rh−S−C_{ax}[c]	−1.8	−10.1
Interplanar Angle, Ω,[d] deg		
	13.7	16.1

[a] For a torsion angle defined by $i-j-k-l$, sign conventions are (+) if a clockwise and (−) if a counterclockwise rotation of the $i-j$ bond vector is required to bring it inline with the $k-l$ vector as one views along the $j-k$ vector. [b] C_{eq} = C(9) (**2a**) and C(12) (**2b**). [c] C_{ax} = C(13) (**2a**) and C(9) (**2b**). [d] Angle between the least-squares planes of the arene and the coordination plane.

Table 2. Crystal Data and Structure Refinement Parameters for **2a** and **2b**

	2a	**2b**
empirical formula	$C_{22}H_{32}S_2ClRh$	$C_{17}H_{25}S_2ClRh$
formula weight	498.96	431.85
crystal system	triclinic	monoclinic
space group	*P*-1	*P*2(1)/*c*
a, Å	9.7415(4)	13.7742(5)
b, Å	10.7597(4)	14.5168(5)
c, Å	11.4033(4)	9.3963(3)
α, deg	104.7330(10)	90
β, deg	92.8090(10)	101.5540(10)
γ, deg	93.9840(10)	90
volume, Å^3	1150.40(8)	1840.79(11)
Z	2	4
D_{calcd}, Mg/m^3	1.440	1.558
abs coeff, mm^{-1}	1.044	1.291
F(000)	516	884
cryst size, mm^3	0.200 × 0.073 × 0.055	0.407 × 0.204 × 0.046
theta range, deg	1.85−27.5	2.06−27.53
reflns collect.	18 095	28 251
ind reflns	5279 [*R*(int) = 0.0626]	4227 [*R*(int) = 0.0425]
completeness, %	99.5	99.7
abs correct.	empirical	empirical
refine. method	F^2	F^2
GOF on F^2	1.002	1.138
final *R* indices	R1 = 0.0376	R1 = 0.0306
[$I > 2\sigma(I)$]	wR2 = 0.0751	wR2 = 0.0694

Both rhodium atoms possess octahedral geometries in which the coordination sphere is composed of the *mer*-R(SCS) ligand, an axially coordinated hydride, and two bridging chloride ligands. These are the only reported crystallographic structures of (SCS)Rh−pincer complexes to date; thus, direct comparison of bond distances and bond angles to previously reported structures is not possible. Fortunately, several structures of R(PCP)Rh are presently available for comparison with the structures obtained herein. Two structures, ^{t}Bu(PCP)Rh(H)Cl[1c] and ^{t}Bu (PCP)Rh(CH_3)-Cl,[13] possess square pyramidal coordination geometries, and three structures *trans*-Cy(PCP)RhCl_2(L) (L = H_2O, MeOH, EtOH) are octahedral.[2e] The average Rh−C_{ipso} observed here, 1.985(7) Å, is slightly shorter than either of the two R(PCP)Rh complexes (average 2.007(11) Å), but is within the average observed for the octahedral complexes (1.999(13) Å). The observed Rh−Cl_{eq} (chloride trans to C_{ipso}) distance is 2.508(3) Å and is significantly longer than the average Rh−Cl distance of 2.448(33) Å for the two ^{t}Bu(PCP)Rh-(R′)Cl structures. This comes as no surprise considering that the chlorides for **2** bridge the two rhodium centers. The average rhodium−hydride distance of 1.45(5) Å is in agreement with the average Rh−H distance (1.5(1) Å) observed from other crystallographically determined rhodium−hydride complexes.[15] Finally, the average Rh−S distance observed for **2a** and **2b**, 2.308(15) Å, is slightly shorter than other Rh(III) complexes containing trans-ligated thioethers (2.346(19) Å, N = 13).[16] This reduced distance is a consequence of the confined pendant ligands within the pincer framework.

The alkyl groups of both **2a** and **2b** occupy either axial (ax) or equatorial (eq) positions. An adequate measure of the positioning of the alkyl groups is the torsional angle (ω, H−Rh−S−C) between the hydride and the tertiary carbon (**2a**) or the secondary carbon (**2b**) of the alkyl substituent. The torsional angles for the equatorial substituents are approximately 40° (depending upon the view), but those of the axial substituents are quite different. The measured values of ω for the axial substituents of **2a** and **2b** are −1.8° and −10.1°, respectively. Since there was no detectable disorder present in the alkyl substituents, this difference must be attributable to conformational differences between the two five-membered rings. The conformation of the bicyclic system and the thioether substituents deserves mentioning.

Common to all pincer complexes, there exists a twist about the C_{ipso}−M bond such that one-third of the arene resides above the coordination plane and the other third lies below (Figure 1). Estimation of the extent of puckering is possible

(15) (a) Crocker, C.; Errington, R. J.; McDonald, W. S.; Odell, K. J.; Shaw, B. L.; Goodfellow, R. J. *J. Chem. Soc., Chem. Commun.* **1979**, 498−499. (b) Kovalev, I. P.; Erdakov, K. V.; Vinogradov, M. G.; Yanovskii, A. I.; Struchkov, Y. T. *Metalloorg. Khim.* **1989**, *2*, 673−676. (c) Rappert, T.; Nurnberg, O.; Mahr, N.; Wolf, J.; Werner, H. *Organometallics* **1992**, *11*, 4156−4164. (d) Wang, K.; Emge, T. J.; Goldman, A. S.; Li, C. B.; Nolan, S. P. *Organometallics* **1995**, *14*, 4929−4936. (e) van der Boom, M. E.; Liou, S.-Y.; Ben-David, Y.; Gozin, M.; Milstein, D. *J. Am. Chem. Soc.* **1998**, *120*, 13415−13421. (f) Hahn, C.; Spiegler, M.; Herdtweck, E.; Taube, R. *Eur. J. Inorg. Chem.* **1998**, 1425−1432.

(16) (a) McCrindle, R.; Ferguson, G.; McAlees, A. J.; Parvez, M.; Ruhl, B. L.; Stephenson, D. K.; Wieckowski, T. *J. Chem. Soc., Dalton Trans.* **1986**, 2351−2359. (b) Ferguson, G.; Matthes, K. E.; Parker, D. *Angew. Chem., Int. Ed. Engl.* **1987**, *26*, 1162−1163. (c) Clark, P. D.; Machin, J. H.; Richardson, J. F.; Dowling, N. I.; Hyne, J. B. *Inorg. Chem.* **1988**, *27*, 3526−3529. (d) Helps, I. M.; Matthes, K. E.; Parker, D.; Ferguson, G. *J. Chem. Soc., Dalton Trans.* **1989**, 915−920. (e) Blake, A. J.; Reid, G.; Schroder, M. *J. Chem. Soc., Dalton Trans.* **1989**, 1675−1680. (f) Cooper, S. R.; Rawle, S. C.; Yagbasan, R.; Watkin, D. J. *J. Am. Chem. Soc.* **1991**, *113*, 1600−1604. (g) Parvez, M.; Fait, J. F.; Clark, P. D.; Jones, C. G. *Acta Crystallogr., Sect. C: Cryst. Struct. Commun.* **1993**, *49*, 383−385. (h) Gaswami, N.; Alberto, R.; Barnes, C. L.; S., J. *Inorg. Chem.* **1996**, *35*, 7546−7555. (i) Blake, A. J.; Li, W. S.; Lippolis, V.; Schroder, M. *Acta Crystallogr., Sect. C: Cryst. Struct. Commun.* **1998**, *54*, 1410−1413.

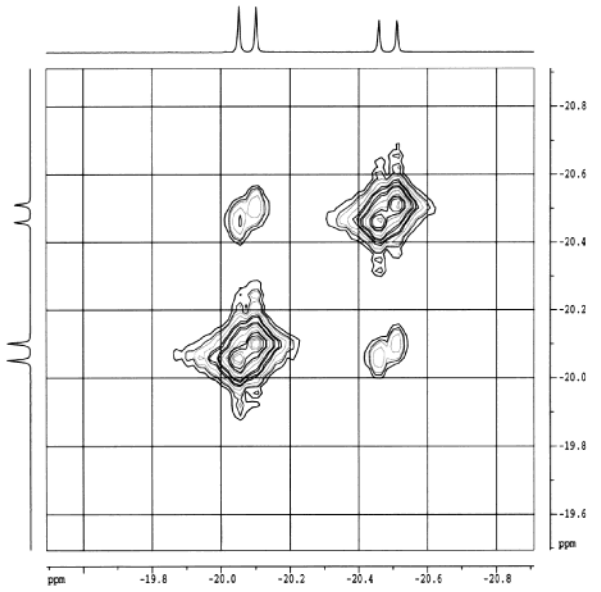

Figure 3. Two-dimensional ^{1}H−^{1}H EXSY (500 MHz, −14 °C, CD_2Cl_2) spectrum of the hydride resonances of diastereomers **A** and **B** of **2a** recorded using a mixing time of 275 ms.

by calculating the interplanar angle (Ω) that exists between the least-squares planes of the arene ring, P_{arene}, and that of the coordination plane, P_{coord}. The values of Ω calculated for **2a** and **2b** are 13.7° and 16.1°, respectively. Thus, the complex with the smaller substituent (^{i}Pr vs ^{t}Bu) shows the largest degree of bicyclic distortion. This may seem to contradict initial expectations as a number of R(SCS)PdCl complexes do indeed show that an increase in the steric bulk of the S substituent results in an increase in Ω.[10,11a,c] However, unlike the R(SCS)PdCl systems, the Rh complexes are dimeric, and as such, the substituent interacts not only with the cyclic ring system, but also with other elements present within the dimer. This is important as the interactions that exist between monomeric pairs control the type of exchange that occurs in solution.

Dynamic Exchange in Solution. Observation of multiple resonances at room temperature in the ^{1}H NMR spectrum that coalesce at higher temperatures suggested that some type of dynamic exchange was operating in solution. Further evidence to support this notion came upon acquisition of two-dimensional (2D) ^{1}H−^{1}H EXSY spectra for **2** in CD_2Cl_2. Figure 3 shows the 2D phase-sensitive ^{1}H EXSY spectrum of **2a** in CD_2Cl_2 at −14 °C.[17] The off-diagonal peaks are of the same phase as the diagonal peaks, indicating that the observed correlation is attributable to chemical exchange and not an NOE (NOE ≡ nuclear Overhauser effect). Careful optimization of the mixing time allowed accurate integration of the relative intensities of the two signals and yielded observed rates of exchange of 0.6 s^{-1} at −14 °C and 12.6 s^{-1} at 24 °C. A similar experiment performed on a sample of **2b** at −30 °C showed that there is a minimum of two exchange networks between different diastereomers in solution, all of which exchange at higher temperatures. Unfortunately, the number of peaks and lack of resolution between them prevented a complete determination of the exchange system. Thus, these experiments substantiate the existence of chemical exchange in solution. The question left remaining is the nature of the exchange process.

Metalated pincer complexes are known to undergo exchange in solution upon rotation about the M−C_{ipso} bond;[11b,18a−c] another exchange process possible for these particular systems is atomic inversion.[11b,18d,f] Since the dimer does not dissociate in solution, the only other conceivable exchange process would be due to pendant thioether dissociation. This is highly unlikely considering the nature of the chelate. Furthermore, experimental evidence, found in the guise of ^{13}C NMR, suggested that this does not occur as both **2a** and **2b** show two-bond Rh−C coupling to the benzylic and S-tethered carbons within the ligand framework. Thus, the problem at hand is to determine which process is operative for **2**, i.e., either Rh−C_{ipso} rotation or sulfur inversion.

Many reports exist that describe the dynamic exchange that occurs in these pincer−metal complexes[11b,18a−d] as well as the fluxional behavior attributable to sulfur inversion.[11b,18,19] In the complex Me(SCS)PdCl,[11b] the authors concluded from the X-ray structure of ^{t}Bu(SCS)PdCl[11a] that the hydrogens α to the point of chelation should be diastereotopic. Indeed, at room temperature, Me(SCS)PdCl displays a single resonance for the benzylic hydrogens, but upon cooling to −40 °C two sets of AB quartets were observed for the benzylic hydrogens, which was attributed to the existence of two diastereomers in solution. The authors reasoned that, in this particular system, the source of exchange was due to either sulfur inversion or rotation about the Pd−C_{ipso} bond, but they were unable to unambiguously determine which pathway was operative. In the case of R(NCN)NiBr, the source of exchange was due solely to M−C_{ipso} bond rotation and was strongly dependent upon the nature of R. For example, in Me(NCN)NiBr,[18a] the benzylic hydrogens appeared as singlets even at −83 °C, but when the two opposing nitrogen substituents were tethered to one another via a poly(methylene) chain, the rate of rotation slowed enough to be a measurable phenomenon.[18b] In addition, the introduction of sterically bulky ligands served to increase the barrier to rotation, thereby permitting measurement of this process.[18c] The presence of two AB quartets of unequal intensity, for the benzylic hydrogens in the ^{1}H NMR spectrum (C_6D_6) of

(17) (a) Perrin, C. L.; Gipe, R. K. *J. Am. Chem. Soc.* **1984**, *106*, 4036−4038. (b) Perrin, C. L.; Dwyer, T. J. *Chem. Rev.* **1990**, *90*, 935−967.

(18) M−C rotation. (a) Grove, D. M.; van Koten, G.; Ubbels, H. J. C.; Zoet, R. *Organometallics* **1984**, *3*, 1003−1009 and references therein. (b) Terheijden, J.; van Koten, G.; van Beek, J. A. M.; Vriesema, B. K.; Kellogg, R. M.; Zoutberg, M. C.; Stam, C. H. *Organometallics* **1987**, *6*, 89−93. (c) van Beek, J. A. M.; van Koten, G.; Dekker: G. P. C. M.; Wissing, E.; Zoutberg, M. C.; Stam, C. H. *J. Organomet. Chem.* **1990**, *394*, 659−678. (d) van Beek, J. A. M.; van Koten, G.; Ramp, M. J.; Coenjaarts, N. C.; Grove, D. M.; Goubitz, K.; Zoutberg, M. C.; Stam, C. H.; Smeets, W. J. J.; Spek, A. L. *Inorg. Chem.* **1991**, *30*, 3059−3068. Sulfur inversion. (e) Orrell, K. G. *Coord. Chem. Rev.* **1989**, *96*, 1−48. (f) Abel, E. W.; Bhargava, S. K.; Orrell, K. G. *Prog. Inorg. Chem.* **1984**, *32*, 1−118.

(19) (a) Abel, E. W.; Moss, I.; Orrell, K. G.; Sik, V. *J. Organomet. Chem.* **1987**, *326*, 187−200. (b) Abel, E. W.; Budgen, D. E.; Moss, I.; Orrell, K. G.; Sik, V. *J. Organomet. Chem.* **1989**, *362*, 105−115. (c) Ascenso, J. R.; Carvalho, M. D.; Dias, A. R.; Romao, C. C.; Calhorda, M. J.; Veiros, L. F. *J. Organomet. Chem.* **1994**, *470*, 147−152.

Scheme 2

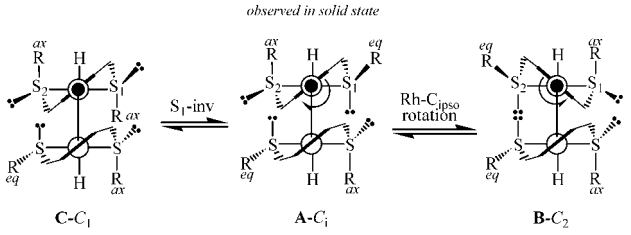

2a, showed that two diastereomers existed in solution and the rate of exchange was slow relative to the NMR time scale.

Scheme 2 represents the two possible equilibria, rotation about the Rh−C_{ipso} bond and sulfur inversion, that are possible for these complexes. The starting point is the Newman projection (**A**) of the observed solid-state structure for **2a** (cf. Figure 1). A clockwise rotation about the Rh(1)−C(1) bond (monomer on top) would result in the formation of a complex **B** that is a diastereomer of **A**. This dimer is C_2 symmetric where the 2-fold axis is perpendicular to and passes through the centroid of the Cl−Rh−Cl′−Rh′ four-membered ring. The alkyl groups remain syn relative to each other, but simply change orientations relative to the two meridonal ligands. The inherent symmetry of both **A** and **B** suggests that both hydrides are magnetically equivalent, and thus this exchange process would yield only two signals. Assuming that sulfur inversion occurs without a concomitant change in the conformation of the ring system,[11b] then inversion at S_1 would result in a species, **C**, which is C_1 symmetric. This process situates one alkyl group anti, relative to the hydride, and produces a complex that exhibits two anisochronous hydrides. Since the data do not support the presence of species **C**, the only observable exchange process in **2a** must be due to rotation about the Rh−C_{ipso} bond.

In the event that both of the processes occur in tandem, then a scheme that includes both sulfur inversion and Rh−C_{ipso} rotation would easily account for the additional hydride resonances observed in **2b**. Evidence to support that the sulfur-inversion pathway is operative in **2b** appears in Figure 4, which corresponds to the ^{1}H NMR spectrum (hydride region) of **2b** in d_8-toluene at 21 °C. The figure identifies 11 unique hydride signals, but careful examination shows several others whose presence is either partially obscured by larger signals or difficult to discriminate from noise. The two predominant peaks (2 and 5) presumably represent the two diastereomers that interconvert via Rh−C_{ipso} bond rotation, as their relative intensities are nearly identical with that observed for **2a** in d_8-toluene (see below). As mentioned above, increasing the temperature of the sample to 88 °C results in the coalescence of all hydride signals (see Supporting Information), and suggests that all of the minor hydride signals represent unique diastereomeric species that readily interconvert on the NMR time scale (400.132 MHz).

The discussion involving Scheme 2 suggested that at least four hydride signals would be possible for the three species present in solution (one each for **A** and **B** and two for **C**). A scheme that accounts for all of the possible diastereomers for **2b** in solution would be prohibitively expansive, and so an abbreviated version appears in Scheme 3. Rather than

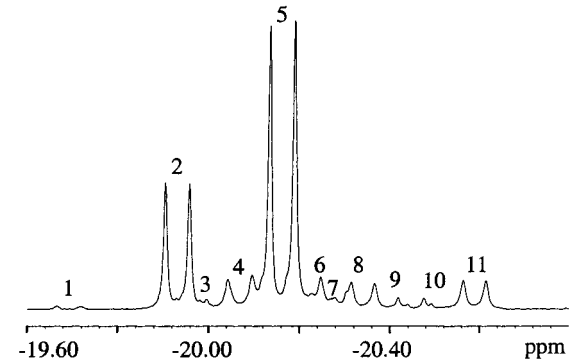

Figure 4. ^{1}H NMR spectrum (hydride region) of **2b** in d_8-toluene at 21 °C.

Scheme 3

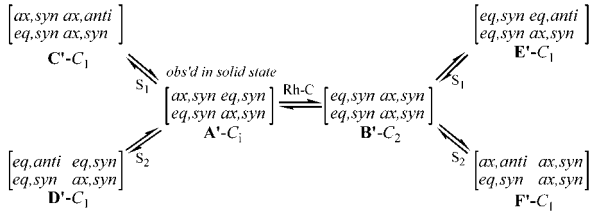

depicting the dimers as Newman projections, a matrix is sufficient to describe the inherent stereochemical properties of each species. The positions of the alkyl groups are denoted as either axial (ax) or equatorial (eq), relative to the metallocycle, and either syn or anti, relative to the hydride. The starting point for the scheme is the centrosymmetric diastereomer **A′** (cf. Figure 2 and Scheme 2) in which the ^{i}Pr groups are either ax or eq, and syn relative to the hydride. Rotation about the Rh−C_{ipso} bond (**A′**→**B′**) simply changes the relative orientations of the alkyl substituents and accounts for the presence of the two predominant signals (2 and 5) shown in Figure 4. Sulfur inversion at S(1) (**A′**→**C′**) and S(2) (**A′**→**D′**) results in the placement of one ^{i}Pr group anti relative to the hydride. These two complexes are diastereomeric, and both would provide two anisochronous hydride signals in the ^{1}H NMR spectrum. (The scheme is simplified by recognition of the fact that inversion of sulfur at either S(1) or S(1A), and either S(2) or S(2A) yields species that are enantiomeric.) Conversely, starting from the C_2-symmetric diastereomer, **B′**, sulfur inversion at either S(1) or S(2) would result in two diastereomeric complexes, **E′** and **F′**. This scheme suggests that at least 10 hydride resonances are possible (one signal each for **A′** and **B′**, two signals each for **C′**, **D′**, **E′**, and **F′**). Obviously, a more complex scheme could easily account for additional resonances as rotation about the Rh−C_{ipso} bond could occur for **C′**, **B′**, **E′**, and **F′**. Schematic accuracy aside, rationalization of the additional hydride resonances observed for **2b** must include both dynamic processes.

Suppression of the atomic inversion pathway in **2a** must be a consequence of the increase in steric bulk of the ^{t}Bu substituent. Scheme 4 depicts the Newman projections of the undetected intermediates that would occur in **2** for either Rh−C_{ipso} rotation (**I**) or sulfur inversion (**II**). Rotation around the metal−carbon bond situates both alkyl groups in pseudo-equatorial positions (peq) while the sulfur atoms retain

Scheme 4

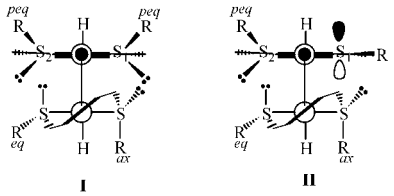

tetrahedral geometry. A two-point estimation of the activation parameters, as provided by the determined rate constants via EXSY experiments, for the process (**A** → **I** → **B**; Schemes 2 and 4) observed for **2a** yielded $\Delta H^{\ddagger}$ and $\Delta S^{\ddagger}$ values of 12 kcal mol^{-1} and −13 cal mol^{-1} K^{-1}, respectively. These values provide some insight into the nature of this process, which is an inherent characteristic of all pincer−metal chelates. The enthalpic penalty of about 12 kcal mol^{-1} is in agreement with expectations when one considers that rotation about the Rh−C$_{ipso}$ bond results in a reduction of Ω, and would naturally lead to a lengthening of this bond length. The observed value of −13 eu for $\Delta S^{\ddagger}$ is presumably a baseline measure of the eclipsing interactions that exist between the ^{t}Bu substituents and the benzylic hydrogens. The intermediate formed upon inversion at S(1), **II**, is very similar to **I** with the exception that the sulfur becomes trigonal planar and the alkyl group resides within the coordination plane. Considering that the distance between the two opposing sulfurs is only ca. 4.1 Å, it becomes apparent why this process does not occur in **2a** as there must be prohibitive steric interactions that exist between the ^{t}Bu and either the equatorially coordinated chloride or the opposing sulfur lone pair or both. Apparently, the ^{i}Pr group is capable of overcoming these geometrical restrictions by accessing a rotamer that directs the methyl groups away from the sterically congested environment.

Considering that **2a** exhibits only a single dynamic exchange process, is it possible to assign the two hydride resonances? The symmetry differences of both **A** and **B** suggest that the latter would possess a dipole moment and that perturbation of the equilibrium would occur upon variation of the dielectric of the solvent. Figure 5 contains the hydride region of **2a** in four different solvents (CD_2Cl_2, *o*-$Cl_2C_6D_4$, d_8-toluene, and d_6-benzene) where **A** denotes the upfield hydride resonance. There exists a strong solvent dependence, as the ratio between the two (**A**/**B**) increases upon a decrease in the dielectric constant of the solvent. The integrated intensities of the two hydride signals are nearly equal in CD_2Cl_2, but become unequal upon a decrease in the solvent polarity. Based on these observations, the upfield resonance is attributable to the low-polarity diastereomer, **A**.

Finally, a system undergoing a two-site exchange provides an opportunity to determine the apparent equilibrium constant between the two species. Variable-temperature ^{1}H NMR in CD_2Cl_2 from −82 to 24 °C showed that the downfield resonance is nearly 3 times more abundant than that of **A** at −82 °C. Careful integration of the hydride signals afforded an apparent equilibrium constant (K_{app} = **B**/**A**) at each temperature and provided an opportunity to subject these data to a van't Hoff analysis. This resulted in the following values,

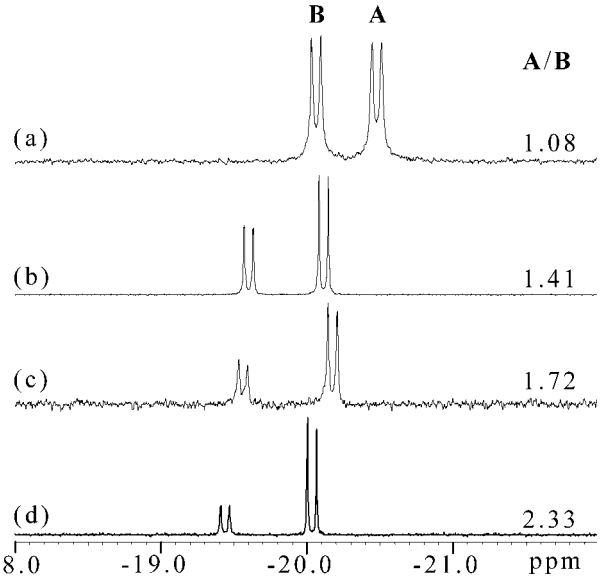

Figure 5. Hydride region of [^{t}Bu(SCS)Rh(H)Cl]$_2$ at 24 °C in (a) CD_2Cl_2, (b) d_4-1,2-dichlorobenzene, (c) d_8-toluene, and (d) d_6-benzene.

for the **A**−**B** equilibrium: $\Delta H = -1.0 \pm 0.1$ kcal mol^{-1} and $\Delta S = -3.3 \pm 0.6$ cal mol^{-1} K^{-1}. The preference of **B** with respect to **A** at lower temperatures in CD_2Cl_2 is a consequence of the reduced contribution of the $T\Delta S$ term, and is perhaps suggestive of the ability of the solvent to stabilize the dipole moment of the former in solution.

Conclusions

Pincer complexes containing pendant thioether linkages form stable adducts with Rh(III). Unlike the phosphine−pincer complexes, the R(SCS) complexes are dimeric both in the solid state and in solution. The ^{1}H NMR spectra are somewhat complex due to the dynamic exchange, but variable-temperature one-dimensional and EXCSY ^{1}H NMR experiments established that dynamic exchange was operative for both **2a** and **2b**. Literature precedent indicated that the source of this exchange was either due to rotation about the Rh−C$_{ipso}$ bond or brought about by inversion at sulfur. The steric bulk of the *tert*-butyl substituents of **2a** prohibited sulfur inversion, which provided a single source of exchange, Rh−C$_{ipso}$ rotation. The isopropyl substituents present in **2b** apparently are small enough to allow for the existence of both dynamic processes. The presence of these dynamic exchange processes provides a rationale for the absence of literature reports describing the chemistry of the thioether pincer ligands with either Rh or Ir. One should expect to encounter similarly complex solution behavior for these complexes with smaller alkyl groups. Since the solution behavior of the ^{t}Bu(SCS)−pincer adducts are readily interpretable, our focus in this area will concentrate on this ligand framework. Indeed, preliminary results demonstrate that **2a** participates in anion methathesis reactions with either AgOTf or $AgBF_4$ to provide dimeric complexes as well.[20] These complexes show extraordinary reactivity with alkyl and aryl silanes. Experiments are currently in progress to map out the complete reactivity and solution behavior of these interesting molecules.

Experimental Section

All materials, unless otherwise specified, were obtained from Acros or Aldrich and were used without purification. $[(COE)_2RhCl]_2$ was prepared according to a literature procedure.[21] When necessary, work was performed in a Vacuum Atmospheres drybox or using Schlenk techniques under a nitrogen atmosphere. ^1H and ^{13}C NMR spectra were recorded using a Bruker DRX 400 spectrometer with an operating frequency of 400.132 and 100.625 MHz, respectively. Proton decoupled spectra were recorded and both short- ($^1J_{CH}$) and long-range ($^3J_{CH}$) coupling were observed; however, only $^1J_{CH}$ values were reported. All chemical shifts were reported relative to internal TMS ($CDCl_3$) or relative to solvent residual. FT-IR data were collected using a Nicolet Magna-IR 560 spectrometer employing 1 cm^{-1} resolution. Fast atom bombardment (FAB) mass spectrometry was performed on a VG7070E magnetic sector mass spectrometer. Elemental analyses were performed by Desert Analytics (Tucson, AZ). Electrospray mass spectrometry was operated in the positive-ion mode using a Micromass QTOF II (Beverly, MA). Samples, in methylene chloride, were directly infused using a syringe pump operating at 5 mL/min. High-resolution spectra were recorded with poly−D-alanine as an internal molecular weight standard. X-ray analyses were performed using a Bruker SMART CCD system operating at −80 °C (vide infra).

Preparation of 1,3-(^{t}BuSCH$_2$)$_2$C$_6$H$_4$, 1a. To a flask containing 25 mL of anhydrous DMF, 1.4437 g of NaH (95%; 57.2 mmol) was added. The suspension was stirred thoroughly and then cooled to 0 °C where 6.44 mL of 2-methyl-2-propanethiol (57.2 mmol) was added slowly via a syringe yielding a dark brown solution. The solution was stirred an additional 20 min until gas evolution ceased. 1,3-$(ClCH_2)_2C_6H_4$ (5.00 g, 28.5 mmol/25 mL DMF) was added dropwise to the sodium *tert*-butylthiolate solution. Upon complete addition of dichloro-*m*-xylene, the solution turned cloudy white. The ice bath was removed and the solution heated at 100 °C, with stirring, for 3 h. The reaction was allowed to cool to room temperature and was quenched with 100 mL of H_2O, and an additional 50 mL of $CHCl_3$ was added with mixing. The mixture was separated and the aqueous layer washed twice more with 25 mL portions of $CHCl_3$. The collected $CHCl_3$ solution was then washed with water (5 × 50 mL) to remove DMF. Evaporation of the solvent yielded a yellow oil which was recrystallized using CH_3OH/H_2O (2:1) in a refrigerator. White needles were collected by filtration and dried at 30 °C for 3 days at 5 mTorr. The final isolated yield was 6.61 g (23.4 mmol, 82%). A second crystallization yielded an additional 0.243 g of material, but was slightly yellow in color. ^1H NMR (δ, $CDCl_3$): 7.329 (t, $^3J_{HH}$ = 7.4 Hz, 1H, Ar*H*), 7.219 (s, 1H, Ar*H*), 7.209 (d, $^3J_{HH}$ = 7.4 Hz, 2H, Ar*H*), 3.746 (s, 4H, ArCH_2S), 1.350 (s, 18H, SC(CH_3)$_3$). ^{13}C {^1H} NMR (100.625 MHz, CD_2Cl_2) δ ($^1J_{CH}$): 139.3 (s, $C_{1,3}$), 129.9$_7$ (d, C_5, $^1J_{CH}$ = 156.9 Hz), 128.7 (d, C_2, $^1J_{CH}$ = 160.8 Hz), 127.7 (d, $C_{4,6}$, $^1J_{CH}$ = 159.2 Hz), 43.0 (s, −S*C*(CH$_3$)$_3$), 33.5 (t, ArCH$_2$S−, $^1J_{CH}$ = 139.7 Hz), 31.0 (q, −SC(*C*H$_3$)$_3$, $^1J_{CH}$ = 127.0 Hz). Elemental analysis for $C_{16}H_{26}S_2$ obsd (theor): C, 68.24 (68.02); H, 9.32 (9.28). Melting point (uncorrected): 38.1−38.4 °C.

Preparation of 1,3-(^{i}PrSCH$_2$)$_2$C$_6$H$_4$, 1b. Synthesis of this compound occurred using a procedure similar to that for **1a** with the exception that purification of **1b** proceeded by column chromatography (slurried 60−200 mesh SiO_2; hexane/$CHCl_3$ (70:30); 4 × 30 cm column). The desired product eluted as a pale yellow band, and removal of the hexane/$CHCl_3$ solution resulted in the isolation of a pale yellow liquid. The crude yield (>97% purity) for a 57.1 mmol reaction was 92.7%. Further purification occurred upon distillation (bp = 185−187 °C (5 mTorr)) to yield a colorless liquid. Spectroscopic Data: ^1H NMR (C_6D_6) δ (TMS): 7.326 (s, 1H, Ar*H*), 7.093 (m, 3H, Ar*H*), 3.502 (s, 4H, ArCH_2S^{i}Pr), 2.597 (sept, $^3J_{HH}$ = 6.7 Hz, 2H, SC*H*(CH$_3$)$_2$), 1.084 (d, $^3J_{HH}$ = 6.7 Hz, 12H, SCH(CH_3)$_2$). ^{13}C {^1H} NMR (100.625 MHz, CD_2Cl_2) δ ($^1J_{CH}$): 139.2 (s, $C_{1,3}$), 129.2 (d, C_5, $^1J_{CH}$ = 156.2 Hz), 128.4 (d, C_2, $^1J_{CH}$ = 160.1 Hz), 127.2 (d, $C_{4,6}$, $^1J_{CH}$ = 159.3 Hz), 34.9 (t, Ar*C*H$_2$S−, $^1J_{CH}$ = 139.1 Hz), 34.3 (q, −S*C*H(CH$_3$)$_2$, $^1J_{CH}$ = 139.2 Hz), 23.0 (−SCH(*C*H$_3$)$_2$, $^1J_{CH}$ = 126.9 Hz). HR FAB-MS (MH^+) obsd (theor): 255.1252 (255.1241) (4.3 ppm).

Preparation of [μ-ClRh(H)(^{t}BuSCH$_2$)$_2$C$_6$H$_3$-2,6]$_2$, 2a. To a solution of a 1.435 g (2.00 mmol) of $[Rh(COE)_2Cl]_2$ in 75 mL of dry benzene at 25 °C was added 1.187 g (4.20 mmol) of ^{t}Bu(SCHS) ligand in 5 mL of dry benzene. The solution was stirred for 18 h at 25 °C. The resultant pale yellow solid was filtered, washed with 5 × 5 mL of hexanes, and dried in a vacuum for 24 h. This yielded 1.44 g (85.5%) of **2a.** The combined filtrate and washing solution was evaporated to dryness in vacuo. The residue was washed with 5 × 5 mL of hexanes and dried under vacuum for 24 h. This yielded 0.15 g of the same product. IR (ν_{RhH}, cm^{-1}): KBr 2108, CH_2Cl_2 (NaCl plate) 2113. ^1H NMR: except in the arene ^1H region, two distinct sets of resonances were observed for **A** and **B** (δ, ppm, **A**/**B** = 2.33, C_6D_6): 6.88−6.69 (m, 6H, Ar*H*), **A**: 4.26 and 3.65 (d, $^2J_{HH}$ = 14.5 Hz, 8H, ArCH_2S), 1.41 (s, 36H, *t*-Bu), −20.04 (d, $^1J_{RhH}$ = 25.7 Hz, 2H, Rh*H*); **B**: 4.16 and 3.67 (d, $^2J_{HH}$ = 14.5 Hz, 8H, ArCH_2S), 1.42 (s, 36H, *t*-Bu), −19.44 (d, $^1J_{RhH}$ = 23.2 Hz, 2H, Rh*H*). (δ, ppm, **A**/**B** = 1.72, C_7D_8): 6.18−6.65 (m, 6H, Ar*H*), **A**: 4.12 and 3.65 (d, $^2J_{HH}$ = 14.8 Hz, 8H, ArCH_2S), 1.42 (s, 36H, *t*-Bu), −20.16 (d, $^1J_{RhH}$ = 25.2 Hz, 2H, Rh*H*); **B**: 4.20 and 3.63 (d, $^2J_{HH}$ = 14.4 Hz, 8H ArCH_2S), 1.41 (s, 36H, *t*-Bu), −19.55 (d, $^1J_{RhH}$ = 24.0 Hz, 2H, Rh*H*). (δ, ppm, **A**/**B** = 1.28, 1,2-$Cl_2C_6D_4$ (*o*-DCB)): 7.01−6.92 (m, 6H, Ar*H*), **A**: 4.43 and 4.08 (d, $^2J_{HH}$ = 15.6 Hz, 8H, ArCH_2S), 1.72 (s, 36H, *t*-Bu), −20.02 (d, $^1J_{RhH}$ = 25.2 Hz, 2H, Rh*H*); **B**: 4.48 and 4.07 (d, $^2J_{HH}$ = 15.3 Hz, 8H, ArCH_2S), 1.71 (s, 36H, *t*-Bu), −19.51 (d, $^1J_{RhH}$ = 24.4 Hz, 2H, Rh*H*). (δ, ppm, **A**/**B** = 1.02, CD_2Cl_2): 6.80−6.69 (m, 6H, Ar*H*), **A**: 4.27 and 3.88 (d, $^2J_{HH}$ = 14.8 Hz, 8H, ArCH_2S), 1.47 (s, 36H, *t*-Bu), −20.48 (d, $^1J_{RhH}$ = 25.6 Hz, 2H, Rh*H*); **B**: 4.20 and 3.88 (d, $^2J_{HH}$ = 15.2 Hz, 8H, ArCH_2S), 1.466 (s, 36H, *t*-Bu), −20.07 (d, $^1J_{RhH}$ = 24.4 Hz, 2H, Rh*H*). One set of signals observed for ^{13}C NMR spectrum. ^{13}C {^1H} NMR (100.625 MHz, CD_2Cl_2) δ: 165.27 (d, C_{ipso}, $^1J_{RhC}$ = 33.0 Hz), 146.40 (d, C_{ortho}, $^2J_{RhC}$ = 21.2 Hz), 125.56 (d, C_{para}, $^1J_{CH}$ = 160.3 Hz), 120.91 (d, C_{meta}, $^1J_{CH}$ = 156.5 Hz), 48.51 (d, S*C*(CH$_3$)$_3$, $^2J_{RhC}$ = 24.4 Hz), 43.38 (td, Ar*C*H$_2$S, $^2J_{RhC}$ = 3.5 Hz, $^1J_{CH}$ = 139.2 Hz), 29.86 (q, SC(*C*H$_3$)$_3$, $^1J_{CH}$ = 127.7 Hz). Elemental analysis for **2a**·C_6H_6 obsd (theor): C, 49.81 (49.62); H, 6.37 (6.36). Crystals of **2a** suitable for X-ray were obtained from slow evaporation of solvent from a benzene solution or a 1:3 benzene/CH_2Cl_2 solution. High-resolution ESI-MS (CH_2Cl_2) for **2a** ($C_{32}H_{52}S_4Cl_2Rh_2$≡M) gave as the predominant ion $[M - Cl]^+$. Calculated isotopic mass for $[C_{32}H_{52}S_4ClRh_2]^+$ 805.0750 amu, observed 805.0723 amu (3.4 ppm).

Preparation of [μ-ClRh(H)(^{i}PrSCH$_2$)$_2$C$_6$H$_3$-2,6]$_2$, 2b. Performed in a manner identical to that for **2a**. Isolated yield for a 4.2 mmol reaction of **1b** with 2.0 mmol of $[(COE)_2RhCl]_2$ was 1.304 g, 83.0%. ^1H NMR (d_8-toluene, 90 °C, ppm): 6.690 (br s, 6H, ArH), 4.180 (br s, 4H, ArCH_2S), 3.665 (d, $^2J_{HH}$ = 14.4 Hz, ArCH_2S), 3.044 (br s, 4H, SC*H*(CH$_3$)$_2$), 1.362, 1.313 (2 broad singlets, 24H, SCH(CH_3)$_2$). FT-IR (KBr, cm^{-1}): 2120 (s, Rh−H). Consistent with

(20) Evans, D. R.; Huang, M., Chege, E. W. *Abstracts of Papers*, 221st National Meeting of the American Chemical Society, San Diego, CA, Apr 1−5, 2001; American Chemical Society: Washington, DC, 2001; INOR 699.

(21) Bennett, M. A.; Saxby, J. D. *Inorg. Chem.* **1968**, *7*, 321−325.

the EXSY data, some diastereomers do not readily exchange at ambient temperature, but undergo exchange at elevated temperatures. The following reported signals are those of the major signal observed in the spectrum. ^{13}C {^{1}H} NMR (100.625 MHz, CD_2Cl_2) δ: 166.03 (d, C_{ipso}, $^1J_{RhC}$ = 31.8 Hz), 145.73 (s, C_{ortho}), 128.72 (d, C_{para}, $^1J_{CH}$ = 158.0 Hz), 121.79 (d, C_{meta}, $^1J_{CH}$ = 157.2 Hz), 43.43 (d, S*C*H(CH$_3$)$_2$, $^1J_{CH}$ = 140.4 Hz), 41.51 (t, Ar*C*H$_2$S, $^1J_{CH}$ = 142.1 Hz), 22.25 (q, SC(*C*H$_3$)$_3$, $^1J_{CH}$ = 127.9 Hz). Elemental analysis for **2b**·C$_6$H$_6$ obsd (theor): C, 47.47 (47.28); H, 5.86 (5.83). Crystals of **2b** suitable for X-ray were obtained from slow evaporation of solvent from a benzene solution. High-resolution ESI-MS (CH_2Cl_2) for **2b** ($C_{28}H_{44}S_4Cl_2Rh_2$/M) gave as the predominant ion [M − Cl]$^+$. Calculated isotopic mass for [$C_{28}H_{44}S_4ClRh_2$]$^+$ 782.0124 amu, observed 749.0015 amu (0.9 ppm).

X-ray Analysis. Colorless block crystals with dimensions 0.200 × 0.073 × 0.055 mm^3 (**2a**) and 0.407 × 0.204 × 0.046 mm^3 (**2b**) were placed and optically centered on the Bruker SMART CCD system at −80 °C. The initial unit cell was indexed using a least-squares analysis of a random set of reflections collected from three series of 0.3° wide ω scans (25 frames/series) that were well distributed in reciprocal space. Data frames were collected [M*o* Kα] with 0.2° wide ω scans for 10 s. Five complete ω-scan series, 909 frames, were collected with an additional 200 frames a repeat of the first series for redundancy and decay purposes. The crystal-to-detector distance was 4.973 cm, thus providing a complete sphere of data to $2\theta_{max}$ = 55°. A total of 18 095 (**2a**) or 28 251 (**2b**) reflections were collected and corrected for Lorentz and polarization effects and absorption using Blessing's method as incorporated into the program SADABS[22] with 5279 unique [R(int) = 0.0626] (**2a**) and 4227 unique [R(int) = 0.0425] (**2b**).

Structural Determination and Refinement. All crystallographic calculations were performed on a personal computer (PC) with dual Pentium 450 MHz processors and 384 MB of extended memory. The SHELXTL[23] program package, XPREP, was now implemented to determine the probable space group and to set up the initial files. System symmetry indicated the unique centrosymmetric triclinic space group P-1 (no. 2) for **2a** and the monoclinic space group $P2(1)/c$ (no. 14) for **2b**. The structure was determined by direct methods with the successful location of nearly all atoms using the program XS.[24] The structure was refined with XL.[25]

After the initial refinement difference Fourier cycle, additional atoms were located and included within the connectivity table. After several of these refinement difference Fourier cycles, all of the atoms were refined isotropically and then anisotropically. Except for the hydride ligands, all hydrogen atoms were placed in calculated positions. The final structure (**2a**) was refined to convergence [$\Delta/\sigma \leq 0.001$] with $R(F)$ = 5.93%, wR(F^2) = 8.12%, GOF = 1.002 for all 5279 unique reflections [$R(F)$ = 3.76%, wR(F^2) = 7.51% for those 3906 data with $F_o > 4\sigma(F_o)$]. The final structure (**2b**) was refined to convergence [$\Delta/\sigma \leq 0.001$] with $R(F)$ = 4.45%, wR(F^2) = 7.88%, and GOF = 1.138 for all 4227 unique reflections [$R(F)$ = 3.06%, wR(F^2) = 6.94% for those 3128 data with $F_o > 4\sigma(F_o)$]. A final difference Fourier map was featureless, indicating that the structure is therefore both correct and complete.

The function minimized during the full-matrix least-squares refinement was $\sum w(F_o^2 - F_c^2)$, where $w = 1/[\sigma^2(F_o^2) + (\alpha P)^2 + \beta P]$ and $P = (\max(F_o^2,0) + 2F_c^2)/3$ (**2a**: α = 0.0314, β = 0.00; **2b**: α = 0.0337, β = 1.65). An empirical correction for extinction was attempted but was found to be negative and therefore was not applied.

Acknowledgment. Acknowledgment is made for the financial support provided through the Petroleum Research Fund as administered by the American Chemical Society.

Supporting Information Available: Stacked plots of the variable-temperature ^{1}H NMR of **2b** recorded in d_8-toluene, and figures containing the low-resolution ESI-MS of **2a** and **2b** in CH_2Cl_2. Crystal structure data for **2a** (additional molecular structure of **2a**·2CH_2Cl_2) and **2b** including tables of atomic parameters, anisotropic thermal parameters bond distances and bond angles. This material is available free of charge via the Internet at http://pubs.acs.org.

IC011189Y

(22) (a) Blessing, R. H. *Acta Crystallogr.* **1995**, *A51*, 33−38. (b) Sheldrick, G. M. *SADABS* '*Siemens Area Detector Absorption Correction*'; University of Göttingen: Göttingen, Germany, 1996.
(23) Sheldrick, G. M. *SHELXTL/PC*, version 5.03; Siemens Analytical X-ray Instruments, Inc.: Madison, WI, 1994.
(24) Sheldrick, G. M. *Acta Crystallogr., Sect. A* **1990**, *A46*, 467−473.
(25) Sheldrick, G. M. *Shelxl93 Program for the Refinement of Crystal Structures*; University of Göttingen: Göttingen, Germany, 1993.